Supporting Information

Scalable and automated fabrication of conductive tough-hydrogel microfibers with ultra-stretchability, 3D printability and stress-sensitivity

Shanshan Wei[1#], Gang Qu[1#], Guanyi Luo[1#], Yuxing Huang[2], Huisheng Zhang[1], Xuechang Zhou[2], Liqiu Wang[3,4,*], Zhou Liu[2,*], Tiantian Kong[1,4*]

[1]Guangdong Key Laboratory for Biomedical Measurements and Ultrasound Imaging, Department of Biomedical Engineering, School of Medicine, Shenzhen University, Shenzhen, China
[2]College of Chemistry and Environmental Engineering, Shenzhen University, Shenzhen, China
[3]Department of Mechanical Engineering, University of Hong Kong, Hong Kong.
[4]HKU-Zhejiang Institute of Research and Innovation (HKU-ZIRI), Hangzhou, Zhejiang, China.

Correspondence and requests for materials should be addressed to L.Q.W., Z. L. and T. T. K. (email: lqwang@hku,hk, zhouliu@szu.edu.cn; ttkong@szu.edu.cn)

This file contains Supporting Information Note 1-13, Supporting Figures 1-15, Supporting references and full legends for Supporting Movies 1-2.

Supporting Note 1 -The continuous printing of Polyacrylamide (PAA)-graphene oxide (GO) tough-hydrogel microfibers

The PAA-graphene oxide tough-hydrogel microfibers are printed using the similar approach (**Fig. S1 a-b**). The outer aqueous phase consists of graphene oxide (GO, 0.66wt%), acrylamide (AA, 94.56wt%), N,N''-methylenebisacrylamide (MBAA, 1.589wt%), and ammonium persulphate (APS,3.178wt%); the inner phase is 10 wt% $CaCl_2$ aqueous solution. The flow rate ratio of the inner and outer phases is Q_{in}/Q_{out}=5:20, and the printing speed of the translation stage is 1mm/s.

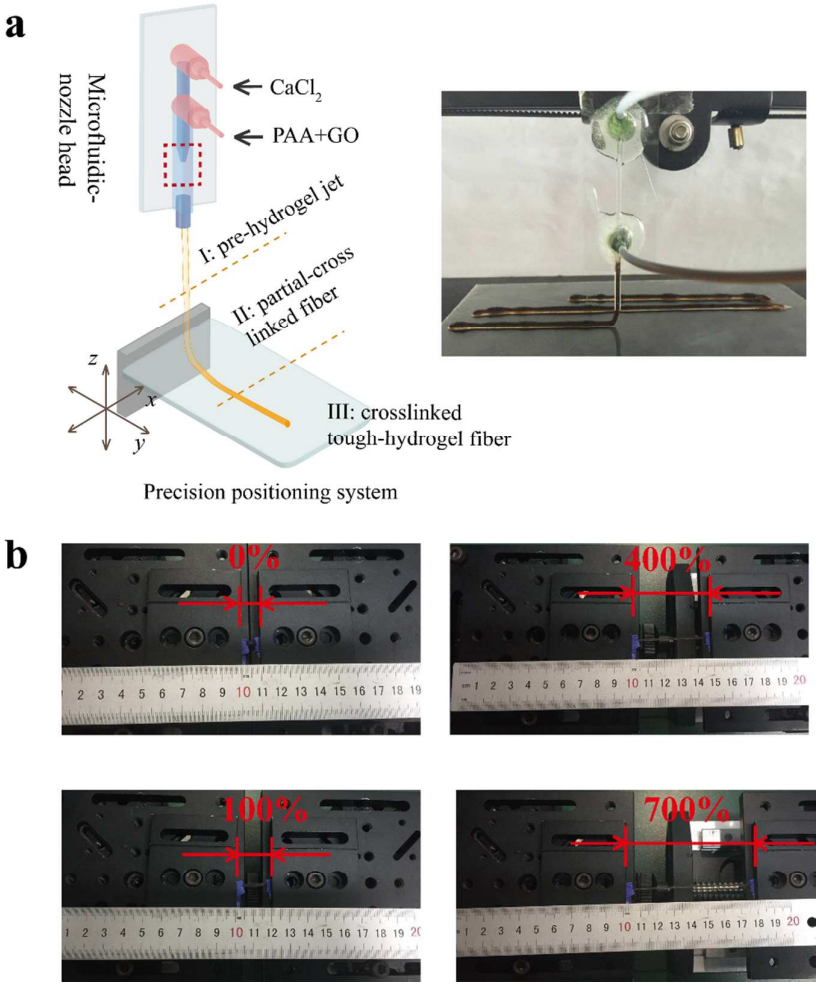

Figure S1. (a) The schematic and image of microfluidic nozzle-head for continuous fabrication and printing PAA-GO tough-hydrogel fibers; (b) Optical images of PAA-GO tough-hydrogel fiber under different stretches: 0%, 100%, 400% and 700%. The original length of microfiber are 1 cm.

Supporting Note 2 -The effect on the water content of the tough-hydrogel microfibers on their toughness

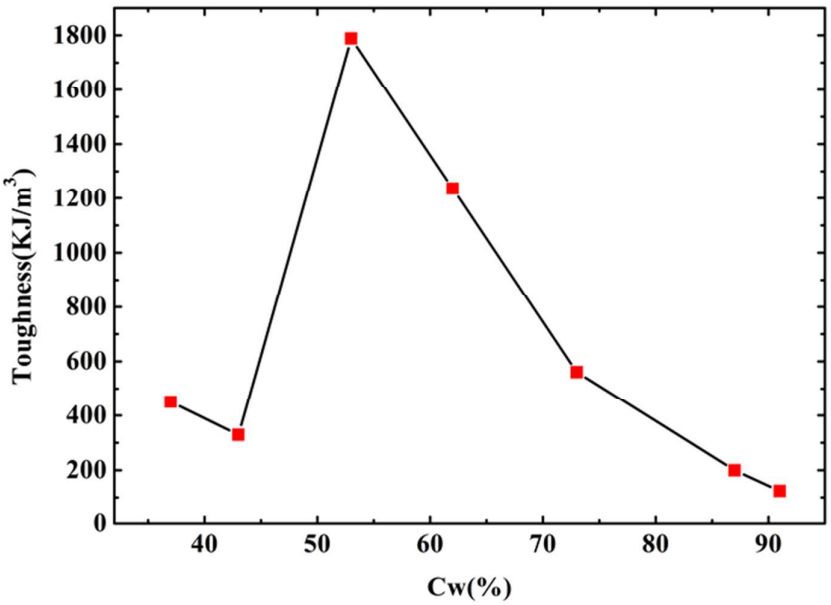

Figure S2. The plot of the calculated toughness (kJ/m^3) as a function of the water content (Cw%) of tough-hydrogel microfibers

Supporting Note 3 -The influence of flow rate ratio Q_{in}/Q_{out} on the stretchability of the resultant PAA-alginate tough-hydrogel microfibers

The mechanical property of the tough-hydrogel microfibers varies as the flow rate ratio of the inner and outer phase Q_{in}/Q_{out} is tuned. The flow rate ratio is optimized to be 3:5 for the largest stretchability of the resultant microfibers (**Fig. S3**).

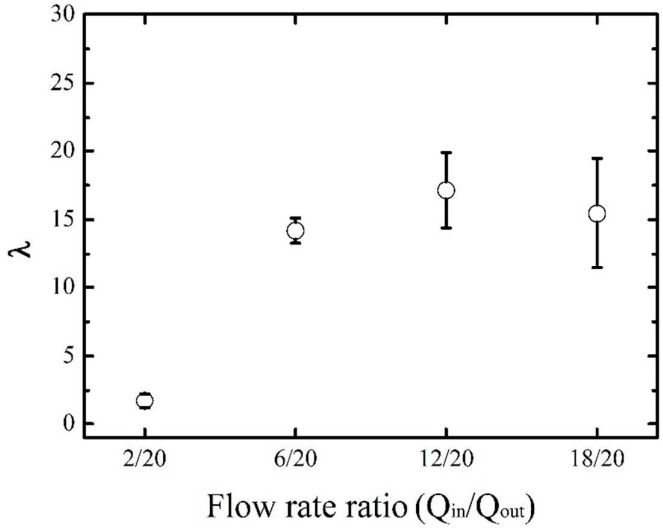

Figure S3. The plot of Q_{in}/Q_{out} as a function of the stretchability (λ) of PAA-alginate tough-hydrogel microfibers

Supporting Note 4 -The effect of the cross-section area of tough-hydrogel microfibers on their stretchability

Under a water content of 65%, when the cross-section area of microfibers is varied from 0.75 mm^2 to 2.75 mm^2, the stretchability, λ=12±3, shows negligible changes (**Fig. S4**). Compared with thick pieces of tough-hydrogels, of which cross-section areas are from 4.8 mm^2 to 12 mm^2, their stretchability are slightly higher, λ=13±2.5 (**Fig. S4**).

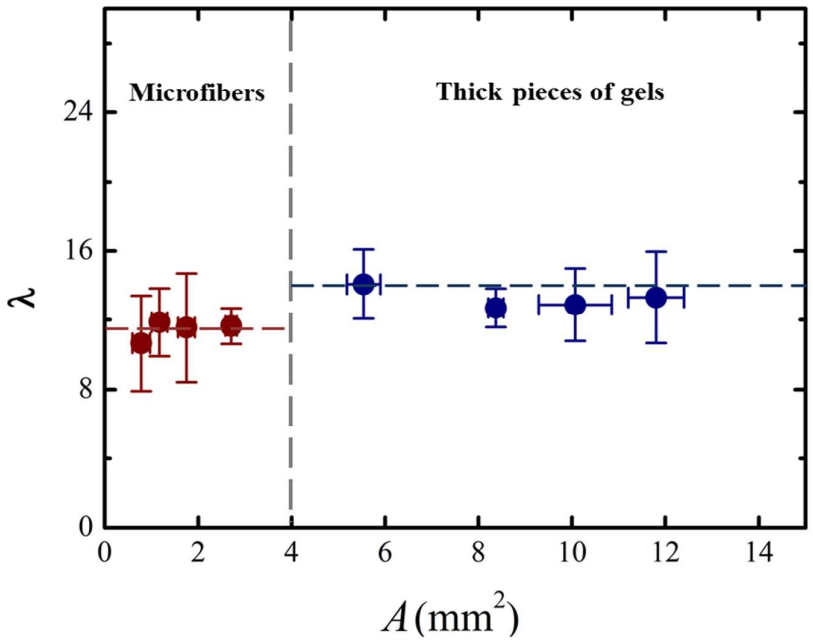

Figure S4. The plot of the cross-section area A (mm^2) as a function of the stretchability (λ) of PAA-alginate tough-hydrogels. The tough-hydrogels with A >4mm^2 are no longer termed as microfibers.

Supporting Note 5 -The the porous structures of the printed tough-hydrogel microfibers

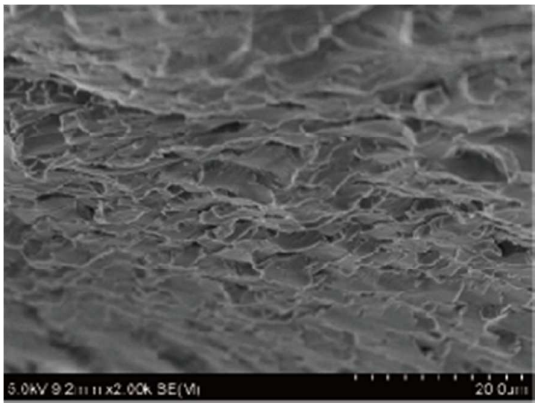

Figure S5. Scanning electronic microscopic (SEM) image showing the porous structures of the printed tough-hydrogel

Supporting Note 6 -The stretchability of the re-hydrated tough-hydrogel microfibers in aqueous solutions

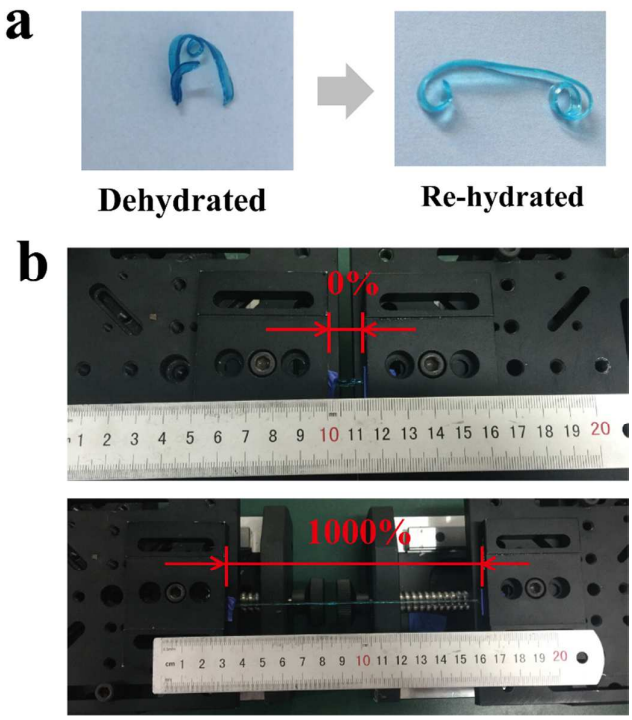

Figure S6. (a) Optic images of dehydrated/dried tough-hydrogel microfibers and rehydrated ones; (b) Optic images showing the rehydrated tough-hydrogel fiber remains ultra-stretchable under 0% and 1000% stretches, respectively. The original length of microfiber are 1.3 cm.

Supporting Note 7 - The effect on the water content of the tough-hydrogel microfibers on their electrical resistivity

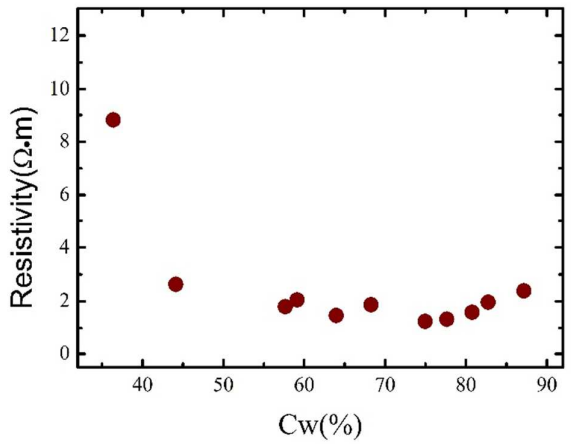

Figure S7. The plot of the measured resistivity (Ω·m) as a function of the water content (Cw%) of tough-hydrogel microfibers

Supporting Note 8 - The schematic of measuring electrical resistance of the tough-hydrogel microfibers

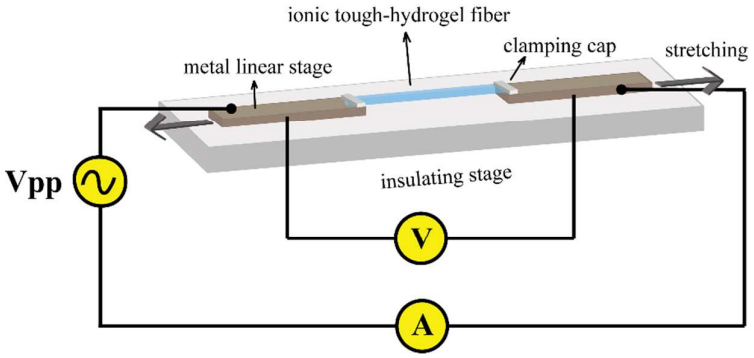

Figure S8. The schematic showing the measure of electrical resistance of the tough-hydrogel fibers with and without the electrolytes, while stretching. The basic design places the tough-hydrogel fiber, the ends of which are bonded on two metal linear stages, on an insulating substrate.

Supporting Note 9 - The linear current-voltage relationships of the tough-hydrogel microfibers

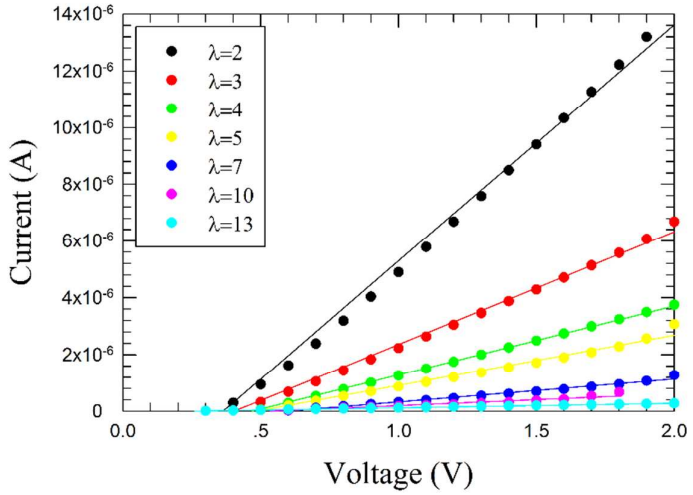

Figure S9. A plot of the measured currents against applied voltages for ionic tough-hydrogel fibers during stretching, using the set-up as shown in Fig. S3. The electrical behaviors of the stretched tough-hydrogel fibers remain omhic, as indicated by the linear fitting with exponent of 1, as the voltage is larger than 0.3 V. The different colors correspond to fibers of different stretches.

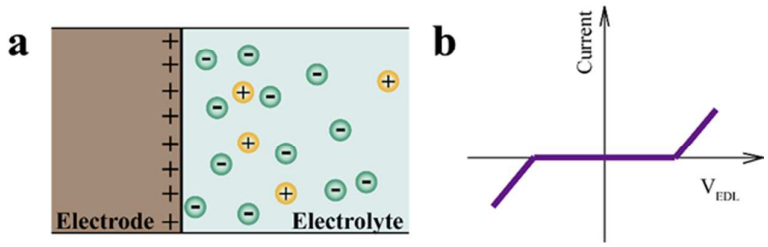

Figure S10. (a) The schematic showing that the electrode/electrolyte interface forms an electrical double layer; (b) When the applied voltage is below certain value, electrons and ions do not across the interface, and thus no electrochemical reaction occurs. The electrical double layer behaves like a capacitor. From reference 1. Reprinted with permission from AAAS.

Supporting Note 10 - The effect of electrolyte concentrations on the stretchability of re-hydrated tough-hydrogel microfibers

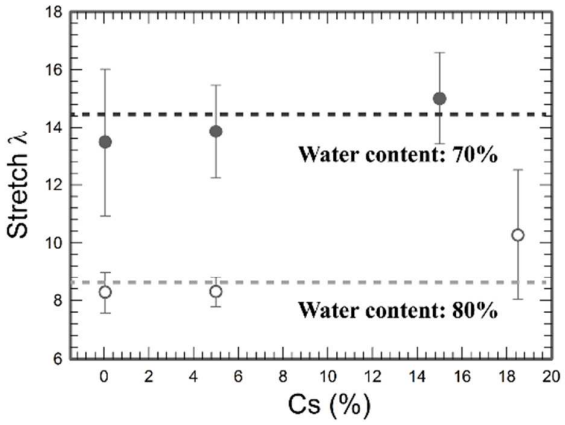

Figure S11. The stretchability of the tough-hydrogel fibers is not influenced by different mass ratios of electrolytes

Supporting Note 11 - The egg jump on the printed tough-hydrogel web

Figure S12. Series of optical images showing the egg jump from a height of 1.2m. The egg bounces and stretches the tough-hydrogel web, finally rests on the web.

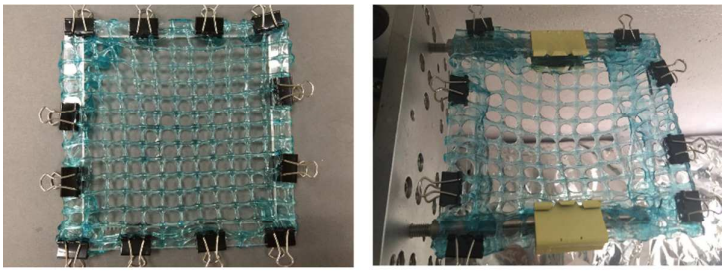

Figure S13. Optical images showing the printed tough-hydrogel web before and after the egg jump. The robustness of the printed web remains intact and stretchable.

Supporting Note 12 - The rheology characterization of PAA-alginate tough-hydrogels

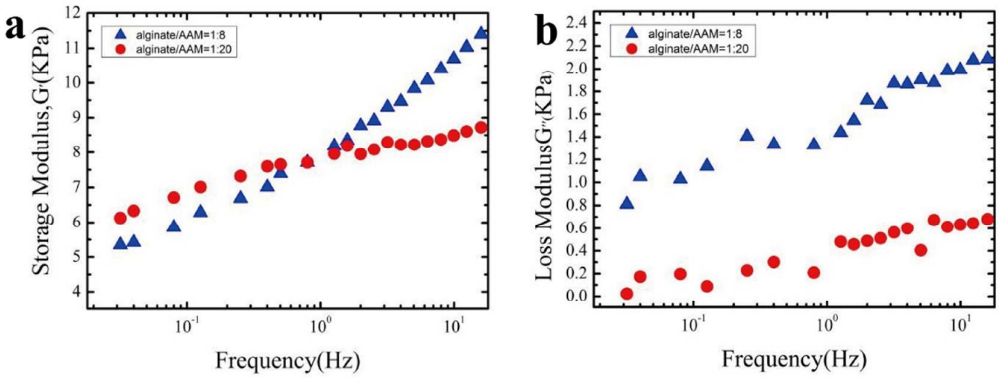

Figure S14. Viscoelasticity of the PAA-alginate tough-hydrogels with different molar mass ratio of alginate to AA, 8:1 and 20:1. (a) Storage modulus G'; (b) Loss modulus G''.

Supporting Note 13 - The stretchability of the PAA-alginate hybrid microfibers with a alginate-to-AA mass ratio of 20:1

The ultra-stretchability of PAA-alginate tough-hydrogels are the following two mechanisms: PAA network maintain its elasticity under large deformation and the reversible Ca^{2+} crosslinking alginate network dissipates mechanical energy[1–6]. As the portion of alginate increases, the elastic modulus of the hybrid hydrogel is decreased and thus the maximum deformation is also decreased[2] (**Fig. S15a-b**).

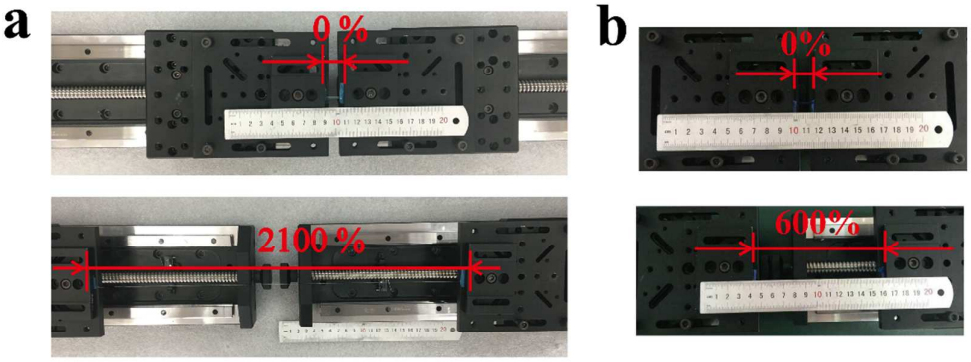

Mass ratio of Alginate:AA=8:1 **Mass ratio of Alginate:AA=20:1**

Figure S15. Optic images showing the maximum stretchability of PAA-alginate tough-hydrogel microfiber with different mass ratios between alginate and AA.

Supporting Movie 1. The lightening up of a series of LED bulbs connected by tough-hydrogel fibers.

Supporting Movie 2. The high-speed video showing the close-up of the egg impacting onto the printed web.

Supporting References

(1) Keplinger, C.; Sun, J.-Y.; Foo, C. C.; Rothemund, P.; Whitesides, G. M.; Suo, Z. Stretchable, Transparent, Ionic Conductors. *Science.* **2013**, *341* (6149), 984–987.

(2) Sun, J.-Y.; Zhao, X.; Illeperuma, W. R. K.; Chaudhuri, O.; Oh, K. H.; Mooney, D. J.; Vlassak, J. J.; Suo, Z. Highly Stretchable and Tough Hydrogels. *Nature* **2012**, *489* (7414), 133–136.

(3) Hong, S.; Sycks, D.; Chan, H. F. ai; Lin, S.; Lopez, G. P.; Guilak, F.; Leong, K. W.; Zhao, X. 3D Printing: 3D Printing of Highly Stretchable and Tough Hydrogels into Complex, Cellularized Structures. *Adv. Mater.* **2015**, *27* (27), 4035-4040.

(4) Yuk, H.; Zhang, T.; Lin, S.; Parada, G. A.; Zhao, X. Tough Bonding of Hydrogels to Diverse Non-Porous Surfaces. *Nat. Mater.* **2015**, *15* (2), 190–196.

(5) Gonzalez, M. A.; Simon, J. R.; Ghoorchian, A.; Scholl, Z.; Lin, S.; Rubinstein, M.; Marszalek, P.; Chilkoti, A.; López, G. P.; Zhao, X. Strong, Tough, Stretchable, and Self-Adhesive Hydrogels from Intrinsically Unstructured Proteins. *Adv. Mater.* **2017**, *29* (10), 1-8.

(6) Lin, S.; Yuk, H.; Zhang, T.; Parada, G. A.; Koo, H.; Yu, C.; Zhao, X. Stretchable Hydrogel Electronics and Devices. *Adv. Mater.* **2016**, *28* (22), 4497–4505.

(7) Yuk, H.; Zhang, T.; Parada, G. A.; Liu, X.; Zhao, X. Skin-Inspired Hydrogel–elastomer Hybrids with Robust Interfaces and Functional Microstructures. *Nat. Commun.* **2016**, *7* (May), 12028.